

Machine Learning the Hubble Constant

Carlos Bengaly^{1,*}, Maria Aldinez Dantas^{2,†}, Luciano Casarini^{3,‡} and Jailson Alcaniz^{1,§}

¹*Observatório Nacional, 20921-400, Rio de Janeiro, RJ, Brazil*

²*Departamento de Física, Universidade do Estado do Rio Grande do Norte, 59610-210, Mossoró - RN, Brazil and*

³*Departamento de Física, Universidade Federal de Sergipe, 49000, São Cristóvão - SE, Brazil*

(Dated: September 20, 2022)

Local measurements of the Hubble constant (H_0) based on Cepheids e Type Ia supernova differ by $\approx 5\sigma$ from the estimated value of H_0 from Planck CMB observations under Λ CDM assumptions. In order to better understand this H_0 tension, the comparison of different methods of analysis will be fundamental to interpret the data sets provided by the next generation of surveys. In this paper, we deploy machine learning algorithms to measure the H_0 through a regression analysis on synthetic data of the expansion rate assuming different values of redshift and different levels of uncertainty. We compare the performance of different algorithms as Extra-Trees, Artificial Neural Network, Extreme Gradient Boosting, Support Vector Machines, and we find that the Support Vector Machine exhibits the best performance in terms of bias-variance tradeoff, showing itself a competitive cross-check to non-supervised regression methods such as Gaussian Processes.

I. INTRODUCTION

The standard model of Cosmology consists of a flat, homogeneous and isotropic universe whose energy content is dominated by a cosmological constant (Λ) and cold dark matter (Λ CDM). Such a model provides the best description of cosmological observations such as temperature fluctuations of the Cosmic Microwave Background (CMB) [3], luminosity distances to Type Ia Supernovae (SNe) [4], large-scale clustering of galaxies (LSS), and weak gravitational lensing (WL) [5–8]. Despite its tremendous success, this model presents theoretical caveats, such as the value of the vacuum energy density [9, 10], in addition to observational challenges e.g. the $\simeq 5\sigma$ Hubble Constant tension between CMB and SNe observations [11–13], as well as milder tensions between matter density perturbation estimates from CMB and LSS, and slightly enhanced CMB lensing amplitude than predicted by the Λ CDM model. These conflicting measurements may hint at physics beyond the standard cosmology.

Given the necessity to probe the Universe at larger and deeper scales, cosmological surveys like J-PAS [14, 15] DESI [16], Euclid [17], SKA [18] and LSST [19] were proposed and developed. They will improve the constraints we currently have on the parameters of the Λ CDM model, and probe departures from it with unprecedented sensitivity. In order to extract the most of cosmological information from the tantalizing amount of data to come, the deployment of machine learning (ML) algorithms on Physics and Astronomy [20, 21] is

becoming crucial to accelerate data processing and improve statistical inference. Some recent applications of ML on Cosmology focuses on reconstructing the late-time cosmic expansion history to constrain dark energy models [22–31], cosmological model discrimination with LSS and WL [32–42], predicting structure formation [43–53], probing the era of reionisation [54–60], photometric redshift estimation [61–68], besides the classification of astrophysical sources [69–72] and transient objects [73–77]. These analyses reveal that ML algorithms are able to recover the underlying cosmology from data and simulations with greater precision than traditionally used techniques e.g. 2-point correlation function and power spectrum, in addition to Markov Chain Monte Carlo (MCMC) methods.

In this paper we discuss the ability to measure the Hubble Constant H_0 from cosmic chronometers measurements ($H(z)$) using different ML algorithms. We first produce $H(z)$ synthetic data-sets with different number of data points and measurement uncertainties, in order to perform a benchmark test of the H_0 constraints for each algorithms given the quality of the input data. Rather than performing a numerical reconstruction across the redshift range probed by the data, and then fitting H_0 , we carry out an extrapolation of the reconstructed $H(z)$ values down to $z = 0$. We also compare their performance with other non-parametric reconstruction methods, such as the popularly adopted Gaussian Processes (GAP) [78]. Our goal is to verify whether they can provide a competitive cross-check with the GAP.

The paper is structured as follows: Section 2 is dedicated to the cosmological framework and the simulations produced for our analysis. Section 3 explains how this analysis is performed, along with the metrics adopted for algorithm performance evaluation. Section 4 presents our results; finally our main conclusions and final remarks are presented in Section 5.

*Electronic address: carlosbengaly@on.br

†Electronic address: aldinezdantas@gmail.com

‡Electronic address: lcasarini@academico.ufs.br

§Electronic address: alcaniz@on.br

II. SIMULATIONS

A. Background cosmology

In order to compare how different predicting algorithm perform with different quality of data, we produce sets of $H(z)$ simulated data sets and adopt the following prescription:

(i) We assume as fiducial cosmology the flat Λ CDM model given by Planck 2018 (TT, TE, EE+lowE+lensing; hereafter P18) [3]:

$$H_0^{\text{fid}} = 67.36 \pm 0.54 \text{ km s}^{-1} \text{ Mpc}^{-1} \quad (1)$$

$$\Omega_m^{\text{fid}} = 0.3166 \pm 0.0084 \quad (2)$$

$$\Omega_\Lambda^{\text{fid}} = 1 - \Omega_m, \quad (3)$$

so that the Hubble parameter follows the Friedmann equation for the fiducial Λ CDM model

$$\left[\frac{H^{\text{fid}}(z)}{H_0^{\text{fid}}} \right]^2 = \Omega_m^{\text{fid}}(1+z)^3 + \Omega_\Lambda^{\text{fid}}. \quad (4)$$

(ii) We compute the values of $H(z)$ considering the N_z data points at an evenly spaced redshift range $0.1 \leq z \leq 1.5$. In order to understand how knowledge of $H(z)$ along the redshift space affects the performance of the statistical learning, we provide different sets of $H(z)$ assuming different numbers of points $N_z = 20, 30, 50$ and 80 .

(iii) We also consider different values of uncertainties for $H(z)$. In particular we assume $\sigma_H(z)/H(z) = 0.008, 0.01, 0.03, 0.05, 0.08$. This variation of $\sigma_H(z)$ allows to evaluate what level of accuracy of measurements of $H(z)$ is necessary in order to obtain a specific precision on the prediction of H_0 .

Such a prescription provides a benchmark to test the performance of the ML algorithms deployed.

B. Uncertainty estimation

Although these algorithms are able to provide measurements of H_0 at a given redshift, they do not provide

```
z_train , z_test , hz_train , hz_test = train_test_split ( z , hz , test_size = 0.25 , random_state = 42 )
```

so that our testing sub-set contains 25% of the original sample size. Then we deploy different ML algorithms on the train test, looking for the “best combination” of

their uncertainties. We develop a Monte Carlo-bootstrap (MC-bootstrap) method for this purpose, described as follows

- Rather than creating a single simulation centered on the fiducial model for each data-set (item (i) of section II), we produce $H(z)$ measurements at a given redshift following a normal distribution centred around its fiducial value according to $\mathcal{N}(H^{\text{fid}}(z), \sigma_H/H)$. $H^{\text{fid}}(z)$ represents the $H(z)$ value given by the fiducial Cosmology, whereas σ_H consists on its uncertainty as described in the item (iii) of section II.
- We repeat this procedure 100 times for each data-set of N_z data-points with σ_H/H uncertainties as described in the item (ii) of section II.
- The 100 MC realisations produced for each case are provided as inputs for the EXT, ANN, XGB and SVM algorithms described in subsection IIIa
- We report the average and standard deviation of these 100 values as the H_0 measurement and uncertainty, respectively, for each N_z and σ_H/H .

III. ANALYSIS

A. Methods

Our regression analyses are carried out with several ML algorithms available in the `scikit-learn` package¹[79]. Firstly we divide our input sample into training and testing data-sets as

hyperparameters with the help of `GridSearchCV`². This

² https://scikit-learn.org/stable/modules/generated/sklearn.model_selection.GridSearchCV.html

function of `scikit-learn`, given a ML method, performs the learning with all the combination of hyperparameters and shows the performance of every combination - or each one of them - during the cross-validation (CV) procedure³. Such a procedure is performed for the sake of avoiding overfitting on the test set. We chose CV = 3 in our analysis, given the limited number of $H(z)$ data-points.

The ML methods deployed in our analysis are given as follows:

- **Extra-Trees (EXT):** An ensemble of randomised decision trees (extra-trees). The goal of the algorithm is to create a model that predicts the value of a target variable by learning simple decision rules inferred from the data features. A tree can be seen as a piecewise constant approximation⁴[80]. We evaluate the algorithm hyperparameter values that best fit the input simulations through a grid search. Hence, our grid search over the EXT hyperparameters are given by:
- **Artificial Neural Network (ANN):** A Multi-layered Perceptron algorithm that trains using backpropagation with no activation function in the output layer⁵[81].
- **Extreme Gradient Boosting (XGB):** A gradient boosting algorithm⁶, which combine the predictions of several base estimators built with a given learning algorithm in order to improve generalisability/robustness over a single estimator [82]. Conversely from averaging methods (e.g. Forest of randomised trees), algorithms such as XGB are built sequentially and one tries to reduce the bias of the combined estimator⁷. Note that XGB is not originally part of the `scikit-learn` package, but uses the same syntax.
- **Support Vector Machines (SVM):** A linear model that creates a line or hyperplane to separate data into different classes [83, 84]. Originally developed for classification problems, it was also extended for regression, as in the goal of this work⁸.

For a detailed description of the *GridSearchCV* deployment on each of these methods, see Appendix A.

³ https://scikit-learn.org/stable/modules/cross_validation.html

⁴ <https://scikit-learn.org/stable/modules/tree.html>

⁵ https://scikit-learn.org/stable/modules/neural_networks_supervised.html

⁶ <https://xgboost.readthedocs.io/en/latest/index.html>

⁷ <https://scikit-learn.org/stable/modules/ensemble.html>

⁸ <https://scikit-learn.org/stable/modules/svm.html>

B. Robustness of results

We define the bias (b) as the average displacement of the predicted Hubble Constant (H_0^{pred}), obtained from the MC-bootstrap method, from the fiducial value, i.e., $\Delta H_0 = H_0^{\text{pred}} - H_0^{\text{fid}}$, and the Mean Squared Error (MSE) as the average squared displacement:

$$b = \langle \Delta H_0 \rangle, \quad \text{MSE} = \langle \Delta H_0^2 \rangle. \quad (5)$$

Using the definition of variance, we estimate the bias-variance tradeoff of our analysis

$$\text{BVT} = \langle \Delta H_0^2 \rangle - \langle \Delta H_0 \rangle^2 = \text{MSE} - b^2, \quad (6)$$

therefore we can evaluate the performance of these algorithms for each simulated data-set specification.

IV. RESULTS

We show our H_0 measurements for each algorithm in Fig. 1. The top panels present the results obtained from the EXT (left) and ANN (right) algorithms, whereas the middle panels display the XGB (left) and SVM (right) results, and the bottom ones show the GAP predictions for the Mat52 and SqExp kernels in the left and right plots, respectively. Each data point at these plots represents the predicted H_0 values (H_0^{pred}) according to the prescription described in Section IIB for each simulated data-set specifications, i.e., different σ_H/H results against the N_z values. The light blue horizontal line corresponds to the fiducial H_0 . We can clearly see that XGB and EXT provide the most stringent constraints among all estimators, but the H_0^{pred} values are not consistent with the fiducial model. This indicates a bias in the results despite the cross-validation procedure adopted to avoid overfitting. We also find that ANN and SVM are able to recover the fiducial H_0 on the cost of larger uncertainties, specially for the former case.

These results show that SVM has the best bias-variance tradeoff among all algorithms, as presented in Fig. IV. We can see that the BVT of SVM is roughly equivalent to those of EXT and XGB for MC simulations assuming $\sigma_H/H = 0.05$ and $\sigma_H/H = 0.08$, but it reduces significantly for realisations with smaller uncertainties. This can be verified in tables I to V, presented in Appendix B, where we tabulate these results along with the training and test set scores. We obtain that SVM provides the smaller difference between these values, indicating that it corresponds to the best performance algorithm.

For the sake of comparison, we show the results obtained with the Gaussian Processes GaPP code [78] using the Squared Exponential (GAP SqExp) and Matérn(5/2) (GAP Mat52) kernels. We find very good

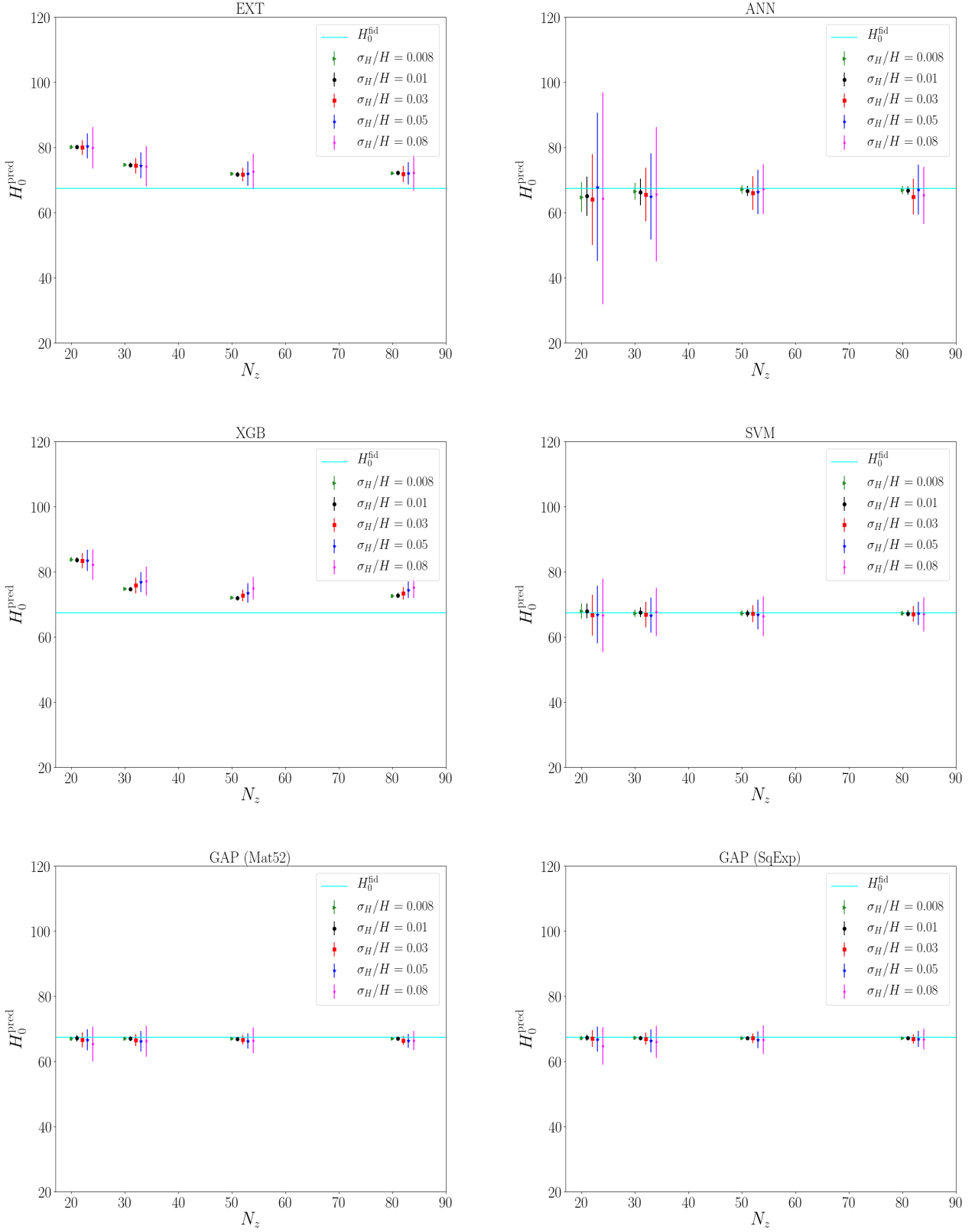


FIG. 1: H_0 measurements from the algorithm EXT (top left), ANN (top right), XGB (center left), SVM (center right), GAP SqExp (lower left) and GAP Mat52 (lower right), plotted against the number of simulated $H(z)$ measurements. Each data point represents different σ_H/H values, whereas the light blue horizontal lines denote the fiducial H_0 value.

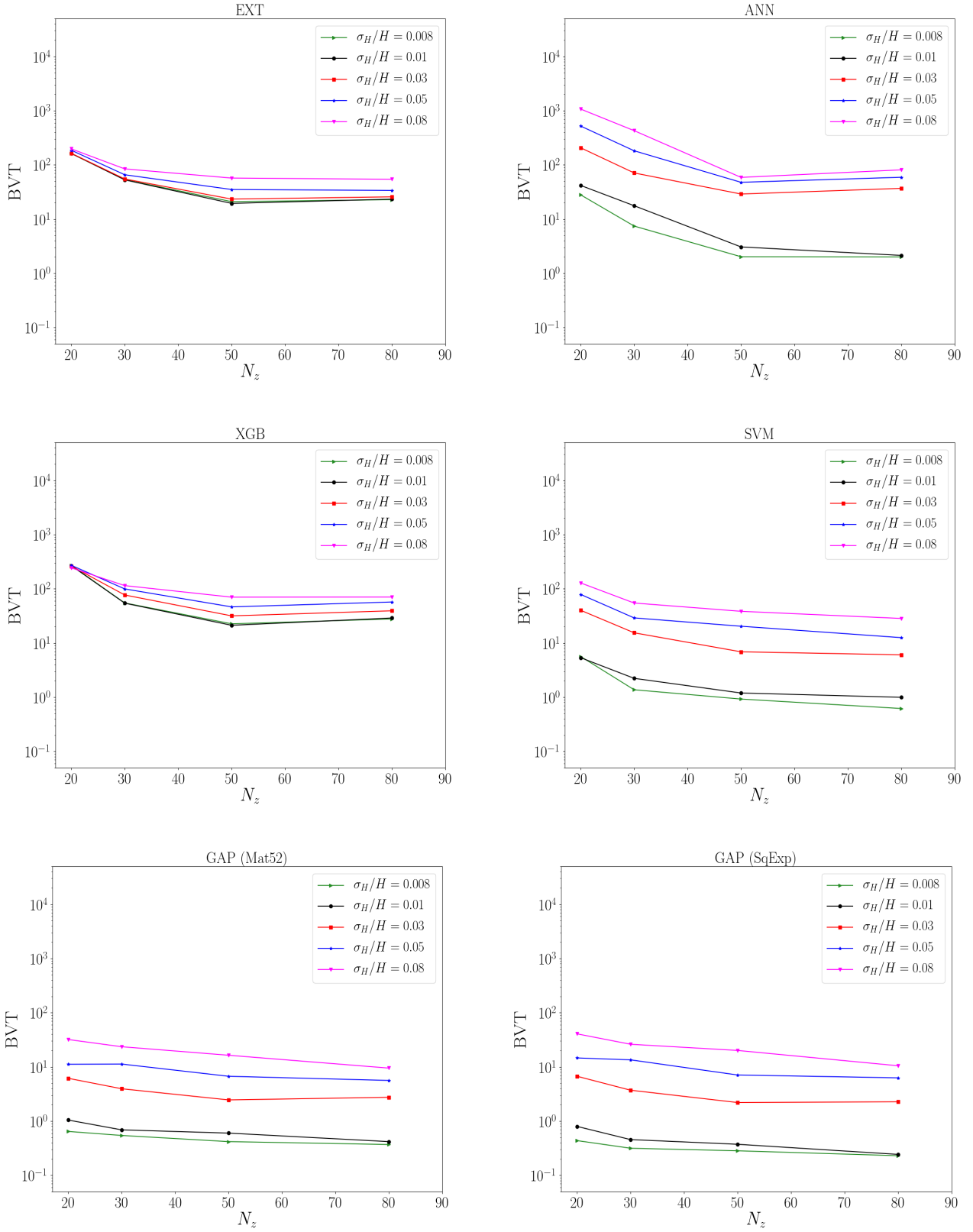


FIG. 2: Same as Fig. 1, but for the BVT. Each data point corresponds to different σ_H/H values.

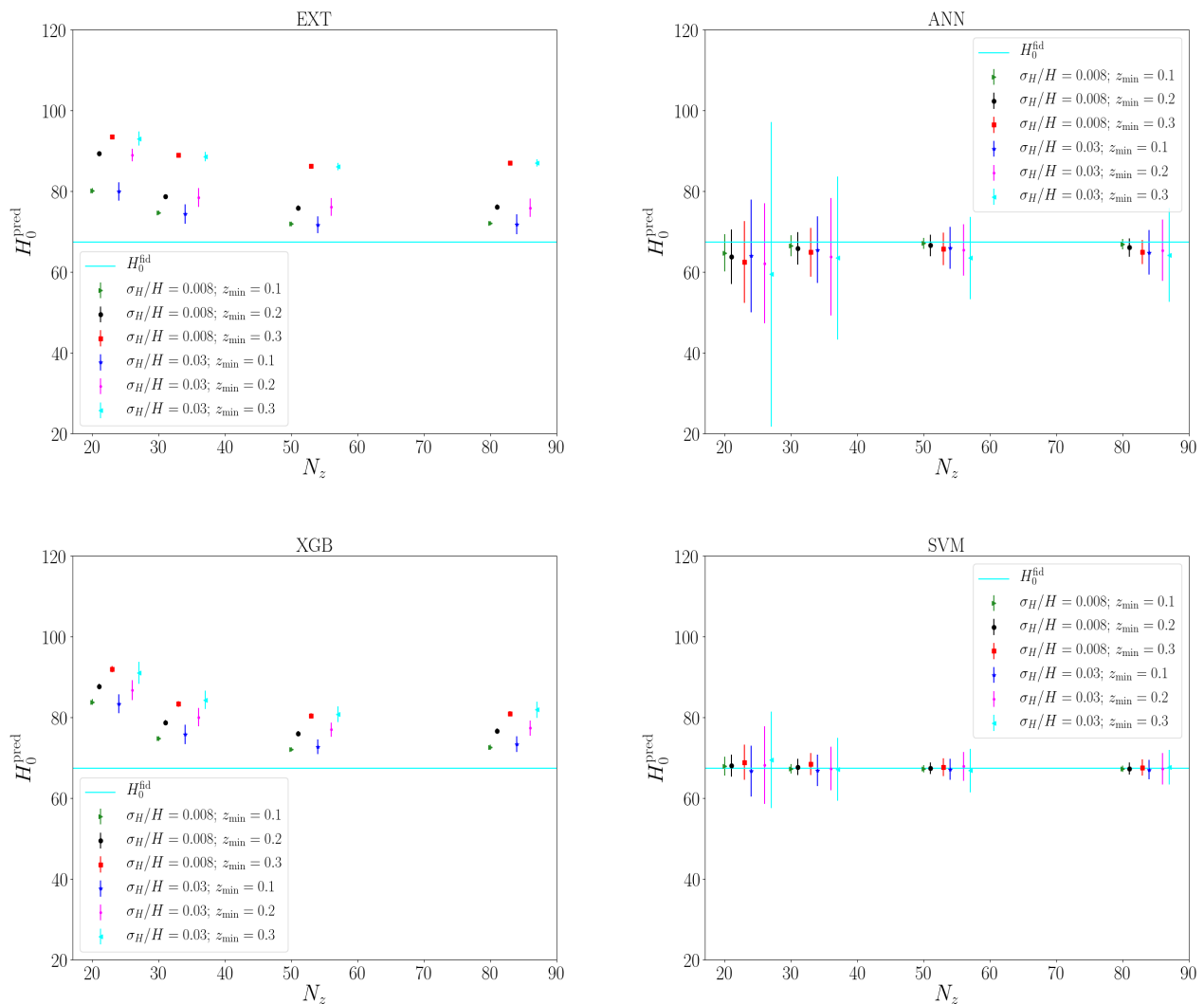


FIG. 3: H_0 measurements obtained using the algorithms EXT (top left), ANN (top right), XGB (bottom left), SVM (bottom right) when assuming different z_{min} values, i.e., $z_{\text{min}} = 0.1, 0.2,$ and 0.3 . This was done for both $\sigma_H/H = 0.008$ and $\sigma_H/H = 0.03$ cases. Again, the horizontal line denotes the fiducial H_0 value.

agreement between the SVM and GAP measurement of H_0 , as well as their respective BVTs. Therefore, we show that SVM can be used as a cross-check method for GAP regression. Moreover, we present H_0 measurements assuming different z_{min} values in Fig. 3, in order to estimate the efficiency of the regression. Again, the SVM presents the best trade-off between variance and bias, thus being the most adequate algorithm to carry out such an analysis. We also verified the results for different cross-validations values, such as $CV = 2, 4, 8$, finding consistent values with those obtained with the standard choice $CV = 3$.

V. CONCLUSIONS

Machine learning has been gaining formidable importance in present times. Given the state-of-art of modern computation and processing facilities, the application of machine learning algorithms in physical sciences not only became popular, but essential in the process of handling huge data-sets and performing model prediction - specially in light of forthcoming redshift surveys.

Our work focused on a comparison of different machine learning algorithms for the sake of measuring the Hubble Constant from cosmic chronometers measurements. We used four different algorithms in our analysis, which are based on decision trees, artificial neural networks, sup-

port vector machine and gradient boosting, as available in the `scikit-learn` python package. We applied them on simulated $H(z)$ data-sets assuming different specifications, and assuming a flat Λ CDM model consistent with Planck 2018 best fit, in order to measure H_0 through an extrapolation procedure.

Our uncertainties are estimated using a Monte Carlo bootstrap method on the simulations, after properly splitting them into training and test sets, and performed a grid search over their hyperparameter space during the cross-validation procedure. In addition, we created a performance ranking between these methods via the bias-variance tradeoff, and compared them with other established methods in the literature, e.g. Gaussian Processes as in the GAPP code.

We obtained that the algorithms based on decision trees and gradient boosting present the lowest performance among all, as they provide low variance with a large bias in the reconstructed H_0 . Instead, the artificial neural networks and support vector machine are able to correctly recover the fiducial H_0 value, where the latter method exhibits the lowest variance among them. We also found that the support vector machine

algorithm presents compatible benchmark metrics with the Gaussian Processes one. This result shows that such method can be successfully used as a cross-check method between different non-parametric reconstruction techniques, which will be of great importance when more precise $H(z)$ measurements become available in the advent of next-generation cosmological surveys.

Acknowledgements

CB acknowledges financial support from the FAPERJ postdoc nota 10 fellowship. LC acknowledges financial support from CNPq (Grant No. 310314/2019-4). J. Alcaniz is supported by Conselho Nacional de Desenvolvimento Científico e Tecnológico CNPq (Grants no. 310790/2014-0 and 400471/2014-0) and Fundação de Amparo à Pesquisa do Estado do Rio de Janeiro FAPERJ (grant no. 233906). We thank the National Observatory Data Center (CPDON) for computational support.

-
- [1] A. G. Riess *et al.* [Supernova Search Team], “Observational evidence from supernovae for an accelerating universe and a cosmological constant,” *Astron. J.* **116** (1998), 1009-1038 [arXiv:astro-ph/9805201].
 - [2] S. Perlmutter *et al.* [Supernova Cosmology Project], “Measurements of Ω and Λ from 42 high redshift supernovae,” *Astrophys. J.* **517** (1999), 565-586 [arXiv:astro-ph/9812133].
 - [3] N. Aghanim *et al.* [Planck Collaboration], “Planck 2018 results. VI. Cosmological parameters,” *Astron. Astrophys.* **641** (2020), A6 [erratum: *Astron. Astrophys.* **652** (2021), C4] [arXiv:1807.06209].
 - [4] D. M. Scolnic *et al.*, “The Complete Light-curve Sample of Spectroscopically Confirmed SNe Ia from Pan-STARRS1 and Cosmological Constraints from the Combined Pantheon Sample,” *Astrophys. J.* **859**, no. 2, 101 (2018) [arXiv:1710.00845].
 - [5] S. Alam *et al.* [eBOSS], “The Completed SDSS-IV extended Baryon Oscillation Spectroscopic Survey: Cosmological Implications from two Decades of Spectroscopic Surveys at the Apache Point observatory,” *Phys. Rev. D* **103** (2021) no.8, 083533 [arXiv:2007.08991].
 - [6] C. Heymans *et al.* “KiDS-1000 Cosmology: Multi-probe weak gravitational lensing and spectroscopic galaxy clustering constraints,” *Astron. Astrophys.* **646** (2021), A140 [arXiv:2007.15632].
 - [7] T. M. C. Abbott *et al.* [DES], “Dark Energy Survey Year 3 Results: Cosmological Constraints from Galaxy Clustering and Weak Lensing,” *Phys. Rev. D* **105** (2022) no.2, 023520 [arXiv:2105.13549].
 - [8] L. F. Secco *et al.* [DES], “Dark Energy Survey Year 3 Results: Cosmology from Cosmic Shear and Robustness to Modeling Uncertainty,” *Phys. Rev. D* **105** (2022) no.2, 023515 [arXiv:2105.13544].
 - [9] S. Weinberg, “The Cosmological Constant Problem,” *Rev. Mod. Phys.* **61**, 1-23 (1989).
 - [10] T. Padmanabhan, “Cosmological constant: The Weight of the vacuum,” *Phys. Rept.* **380**, 235-320 (2003) [arXiv:hep-th/0212290 [hep-th]].
 - [11] E. Di Valentino, O. Mena, S. Pan, L. Visinelli, W. Yang, A. Melchiorri, D. F. Mota, A. G. Riess and J. Silk, “In the realm of the Hubble tension—a review of solutions,” *Class. Quant. Grav.* **38** (2021) no.15, 153001 [arXiv:2103.01183].
 - [12] P. Shah, P. Lemos and O. Lahav, “A buyer’s guide to the Hubble Constant,” *Astron. Astrophys. Rev.* **29** (2021) no.1, 9 [arXiv:2109.01161].
 - [13] A. G. Riess, W. Yuan, L. M. Macri, D. Scolnic, D. Brout, S. Casertano, D. O. Jones, Y. Murakami, L. Breuval and T. G. Brink, *et al.* “A Comprehensive Measurement of the Local Value of the Hubble Constant with 1 km/s/Mpc Uncertainty from the Hubble Space Telescope and the SH0ES Team,” [arXiv:2112.04510].
 - [14] N. Benitez *et al.* [J-PAS], “J-PAS: The Javalambre-Physics of the Accelerated Universe Astrophysical Survey,” [arXiv:1403.5237].
 - [15] S. Bonoli *et al.*, “The miniJPAS survey: a preview of the Universe in 56 colours,” *Astron. Astrophys.* **653**, A31 (2021) [arXiv:2007.01910].
 - [16] A. Aghamousa *et al.* [DESI Collaboration], “The DESI Experiment Part I: Science, Targeting, and Survey Design,” [arXiv:1611.00036].
 - [17] L. Amendola *et al.*, “Cosmology and fundamental physics with the Euclid satellite,” *Living Rev. Rel.* **21**,

- 2 (2018) [arXiv:1606.00180].
- [18] D. J. Bacon *et al.* [SKA Collaboration], “Cosmology with Phase 1 of the Square Kilometre Array: Red Book 2018: Technical specifications and performance forecasts,” *Publ. Astron. Soc. Austral.* **37** (2020), e007 [arXiv:1811.02743].
- [19] D. Alonso *et al.* [LSST Dark Energy Science], “The LSST Dark Energy Science Collaboration (DESC) Science Requirements Document,” [arXiv:1809.01669].
- [20] G. Carleo *et al.*, “Machine learning and the physical sciences,” *Rev. Mod. Phys.* **91**, no.4, 045002 (2019) [arXiv:1903.10563].
- [21] M. Ntampaka *et al.*, “The Role of Machine Learning in the Next Decade of Cosmology,” [arXiv:1902.10159].
- [22] S. Y. Li, Y. L. Li and T. J. Zhang, “Model Comparison of Dark Energy models Using Deep Network,” *Res. Astron. Astrophys.* **19**, 137 (2019) [arXiv:1907.00568].
- [23] R. Arjona and S. Nesseris, “What can Machine Learning tell us about the background expansion of the Universe?,” *Phys. Rev. D* **101** (2020) no.12, 123525 [arXiv:1910.01529].
- [24] C. Escamilla-Rivera, M. A. C. Quintero and S. Capozziello, “A deep learning approach to cosmological dark energy models,” *JCAP* **03**, 008 (2020) [arXiv:1910.02788].
- [25] G. J. Wang, X. J. Ma, S. Y. Li and J. Q. Xia, “Reconstructing Functions and Estimating Parameters with Artificial Neural Networks: A Test with a Hubble Parameter and SNe Ia,” *Astrophys. J. Suppl.* **246**, no.1, 13 (2020) [arXiv:1910.03636].
- [26] G. J. Wang, S. Y. Li and J. Q. Xia, “ECoPANN: A Framework for Estimating Cosmological Parameters using Artificial Neural Networks,” *Astrophys. J. Suppl.* **249** (2020) no.2, 25 [arXiv:2005.07089].
- [27] Y. C. Wang, Y. B. Xie, T. J. Zhang, H. C. Huang, T. Zhang and K. Liu, “Likelihood-free Cosmological Constraints with Artificial Neural Networks: An Application on Hubble Parameters and SN Ia,” *Astrophys. J. Suppl.* **254** (2021) no.2, 43 [arXiv:2005.10628].
- [28] I. Gómez-Vargas, J. A. Vázquez, R. M. Esquivel and R. García-Salcedo, “Cosmological Reconstructions with Artificial Neural Networks,” [arXiv:2104.00595].
- [29] C. García, C. Santa and A. E. Romano, “Deep learning reconstruction of the large scale structure of the Universe from luminosity distance observations,” [arXiv:2107.05771].
- [30] K. Dialektopoulos, J. L. Said, J. Mifsud, J. Sultana and K. Z. Adami, “Neural network reconstruction of late-time cosmology and null tests,” *JCAP* **02**, no.02, 023 (2022) [arXiv:2111.11462].
- [31] P. Mukherjee, J. Levi Said and J. Mifsud, “Neural Network Reconstruction of $H'(z)$ and its application in Teleparallel Gravity,” [arXiv:2209.01113].
- [32] S. Agarwal, F. B. Abdalla, H. A. Feldman, O. Lahav and S. A. Thomas, “PkANN - I. Non-linear matter power spectrum interpolation through artificial neural networks,” *Mon. Not. Roy. Astron. Soc.* **424** (2012), 1409-1418 [arXiv:1203.1695].
- [33] S. Agarwal, F. B. Abdalla, H. A. Feldman, O. Lahav and S. A. Thomas, “pkann - II. A non-linear matter power spectrum interpolator developed using artificial neural networks,” *Mon. Not. Roy. Astron. Soc.* **439** (2014) no.2, 2102-2121 [arXiv:1312.2101].
- [34] S. Ravanbakhsh, J. Oliva, S. Fromenteau, L. C. Price, S. Ho, J. Schneider and B. Poczós, “Estimating Cosmological Parameters from the Dark Matter Distribution,” [arXiv:1711.02033].
- [35] J. Merten, C. Giocoli, M. Baldi, M. Meneghetti, A. Peel, F. Lalande, J. L. Starck and V. Pettorino, “On the dissection of degenerate cosmologies with machine learning,” *Mon. Not. Roy. Astron. Soc.* **487**, no.1, 104-122 (2019) [arXiv:1810.11027].
- [36] A. Peel, F. Lalande, J. L. Starck, V. Pettorino, J. Merten, C. Giocoli, M. Meneghetti and M. Baldi, “Distinguishing standard and modified gravity cosmologies with machine learning,” *Phys. Rev. D* **100**, no.2, 023508 (2019) [arXiv:1810.11030].
- [37] D. Ribli, B. Á. Pataki, J. M. Zorrilla Matilla, D. Hsu, Z. Haiman and I. Csabai, “Weak lensing cosmology with convolutional neural networks on noisy data,” *Mon. Not. Roy. Astron. Soc.* **490**, no.2, 1843-1860 (2019) [arXiv:1902.03663].
- [38] J. Fluri, T. Kacprzak, A. Lucchi, A. Refregier, A. Amara, T. Hofmann and A. Schneider, “Cosmological constraints with deep learning from KiDS-450 weak lensing maps,” *Phys. Rev. D* **100**, no.6, 063514 (2019) [arXiv:1906.03156].
- [39] S. Pan, M. Liu, J. Forero-Romero, C. G. Sabiu, Z. Li, H. Miao and X. D. Li, “Cosmological parameter estimation from large-scale structure deep learning,” *Sci. China Phys. Mech. Astron.* **63** (2020) no.11, 110412 [arXiv:1908.10590].
- [40] M. Ntampaka, D. J. Eisenstein, S. Yuan and L. H. Garrison, “A Hybrid Deep Learning Approach to Cosmological Constraints From Galaxy Redshift Surveys,” [arXiv:1909.10527].
- [41] J. M. Z. Matilla, M. Sharma, D. Hsu and Z. Haiman, “Interpreting deep learning models for weak lensing,” *Phys. Rev. D* **102** (2020) no.12, 123506 [arXiv:2007.06529].
- [42] F. Villaescusa-Navarro, S. Genel, D. Angles-Alcazar, L. Thiele, R. Dave, D. Narayanan, A. Nicola, Y. Li, P. Villanueva-Domingo and B. Wandelt, *et al.* “The CAMELS Multifield Data Set: Learning the Universe’s Fundamental Parameters with Artificial Intelligence,” *Astrophys. J. Suppl.* **259**, no.2, 61 (2022) [arXiv:2109.10915].
- [43] H. M. Kamdar, M. J. Turk and R. J. Brunner, “Machine learning and cosmological simulations – I. Semi-analytical models,” *Mon. Not. Roy. Astron. Soc.* **455** (2016) no.1, 642-658 [arXiv:1510.06402].
- [44] H. M. Kamdar, M. J. Turk and R. J. Brunner, “Machine learning and cosmological simulations – II. Hydrodynamical simulations,” *Mon. Not. Roy. Astron. Soc.* **457** (2016) no.2, 1162-1179 [arXiv:1510.07659].
- [45] L. Lucie-Smith, H. V. Peiris, A. Pontzen and M. Lochner, “Machine learning cosmological structure formation,” *Mon. Not. Roy. Astron. Soc.* **479**, no.3, 3405-3414 (2018) [arXiv:1802.04271].
- [46] S. He, Y. Li, Y. Feng, S. Ho, S. Ravanbakhsh, W. Chen and B. Poczós, “Learning to Predict the Cosmological Structure Formation,” *Proc. Nat. Acad. Sci.* **116**, no.28, 13825-13832 (2019) [arXiv:1811.06533].

- [47] D. K. Ramanah, T. Charnock and G. Lavaux, “Painting halos from cosmic density fields of dark matter with physically motivated neural networks,” *Phys. Rev. D* **100**, no.4, 043515 (2019) [arXiv:1903.10524].
- [48] L. Lucie-Smith, H. V. Peiris and A. Pontzen, “An interpretable machine learning framework for dark matter halo formation,” *Mon. Not. Roy. Astron. Soc.* **490**, no.1, 331-342 (2019) [arXiv:1906.06339].
- [49] M. Tsizh, B. Novosyadlyj, Y. Holovatch and N. I. Libeskind, “Large-scale structures in the Λ CDM Universe: network analysis and machine learning,” *Mon. Not. Roy. Astron. Soc.* **495** (2020) no.1, 1311-1320 [arXiv:1910.07868].
- [50] K. Murakami and A. J. Nishizawa, “Identifying Cosmological Information in a Deep Neural Network,” [arXiv:2012.03778].
- [51] J. Chacón, J. A. Vázquez and E. Almaraz, “Classification algorithms applied to structure formation simulations,” *Astron. Comput.* **38**, 100527 (2022) [arXiv:2106.06587].
- [52] R. von Marttens, L. Casarini, N. R. Napolitano, S. Wu, V. Amaro, R. Li, C. Tortora, A. Canabarro and Y. Wang, “Inferring galaxy dark halo properties from visible matter with Machine Learning,” *Mon. Not. Roy. Astron. Soc.* accepted [arXiv:2111.01185].
- [53] D. Piras, B. Joachimi and F. Villaescusa-Navarro, “Fast and realistic large-scale structure from machine-learning-augmented random field simulations,” [arXiv:2205.07898].
- [54] S. Hassan, A. Liu, S. Kohn and P. La Plante, “Identifying reionization sources from 21 cm maps using Convolutional Neural Networks,” *Mon. Not. Roy. Astron. Soc.* **483** (2019) no.2, 2524-2537 [arXiv:1807.03317].
- [55] N. Gillet, A. Mesinger, B. Greig, A. Liu and G. Ucci, “Deep learning from 21-cm tomography of the Cosmic Dawn and Reionization,” *Mon. Not. Roy. Astron. Soc.* **484** (2019) no.1, 282-293 [arXiv:1805.02699].
- [56] J. Chardin, G. Uhlich, D. Aubert, N. Deparis, N. Gillet, P. Ocvirk and J. Lewis, “A deep learning model to emulate simulations of cosmic reionization,” *Mon. Not. Roy. Astron. Soc.* **490** (2019) no.1, 1055-1065 [arXiv:1905.06958].
- [57] P. La Plante and M. Ntampaka, “Machine Learning Applied to the Reionization History of the Universe in the 21 cm Signal,” *Astrophys. J.* **810** (2019), 110 [arXiv:1810.08211].
- [58] T. Mangena, S. Hassan and M. G. Santos, “Constraining the reionization history using deep learning from 21cm tomography with the Square Kilometre Array,” *Mon. Not. Roy. Astron. Soc.* **494** (2020) no.1, 600-606 [arXiv:2003.04905].
- [59] S. Hassan, S. Andrianomena and C. Doughty, “Constraining the astrophysics and cosmology from 21cm tomography using deep learning with the SKA,” *Mon. Not. Roy. Astron. Soc.* **494** (2020) no.4, 5761-5774 [arXiv:1907.07787].
- [60] D. Prelogović, A. Mesinger, S. Murray, G. Fiameni and N. Gillet, “Machine learning astrophysics from 21 cm lightcones: impact of network architectures and signal contamination,” *Mon. Not. Roy. Astron. Soc.* **509**, no.3, 3852-3867 (2021) [arXiv:2107.00018].
- [61] A. A. Collister and O. Lahav, “ANNz: Estimating photometric redshifts using artificial neural networks,” *Publ. Astron. Soc. Pac.* **116** (2004), 345-351 [arXiv:astro-ph/0311058].
- [62] R. Hogan, M. Fairbairn and N. Seeburn, “GAz: A Genetic Algorithm for Photometric Redshift Estimation,” *Mon. Not. Roy. Astron. Soc.* **449** (2015) no.2, 2040-2046 [arXiv:1412.5997].
- [63] I. Sadeh, F. B. Abdalla and O. Lahav, “ANNz2 - photometric redshift and probability distribution function estimation using machine learning,” *Publ. Astron. Soc. Pac.* **128** (2016) no.968, 104502 [arXiv:1507.00490].
- [64] M. Bilicki *et al.*, “Photometric redshifts for the Kilo-Degree Survey. Machine-learning analysis with artificial neural networks,” *Astron. Astrophys.* **616** (2018), A69 [arXiv:1709.04205].
- [65] Z. Gomes, M. J. Jarvis, I. A. Almosallam and S. J. Roberts, “Improving Photometric Redshift Estimation using GPz: size information, post processing and improved photometry,” *Mon. Not. Roy. Astron. Soc.* **475** (2018) no.1, 331-342 [arXiv:1712.02256].
- [66] G. Desprez *et al.* [Euclid], “Euclid preparation: X. The *Euclid* photometric-redshift challenge,” *Astron. Astrophys.* **644**, A31 (2020) [arXiv:2009.12112].
- [67] L. Cabayol, M. Eriksen, A. Amara, J. Carretero, R. Casas, F. J. Castander, J. De Vicente, E. Fernández, J. García-Bellido and E. Gaztanaga, *et al.* “The PAU survey: estimating galaxy photometry with deep learning,” *Mon. Not. Roy. Astron. Soc.* **506**, no.3, 4048-4069 (2021) [arXiv:2104.02778].
- [68] Kunsági-Máté S., Beck R., Szapudi I. and Csabai I., 2022, “Photometric redshifts for quasars from WISE-PS1-STRM,” [arXiv:2206.01440]
- [69] A. Kurcz, M. Bilicki, A. Solarz, M. Krupa, A. Pollo and K. Małek, “Towards automatic classification of all WISE sources,” *Astron. Astrophys.* **592** (2016), A25 [arXiv:1604.04229].
- [70] E. J. Kim and R. J. Brunner, “Star-galaxy classification using deep convolutional neural networks,” *Mon. Not. Roy. Astron. Soc.* **464** (2017) no.4, 4463-4475 [arXiv:1608.04369].
- [71] R. Beck, I. Szapudi, H. Flewelling, C. Holmberg and E. Magnier, “PS1-STRM: Neural network source classification and photometric redshift catalogue for PS1 3π DR1,” *Mon. Not. Roy. Astron. Soc.* **500**, no.2, 1633-1644 (2020) [arXiv:1910.10167].
- [72] P. O. Baqui *et al.*, “The miniJPAS survey: star-galaxy classification using machine learning,” *Astron. Astrophys.* **645**, A87 (2021) [arXiv:2007.07622].
- [73] M. Lochner, J. D. McEwen, H. V. Peiris, O. Lahav and M. K. Winter, “Photometric Supernova Classification With Machine Learning,” *Astrophys. J. Suppl.* **225** (2016) no.2, 31 [arXiv:1603.00882].
- [74] D. Muthukrishna, D. Parkinson and B. Tucker, “DASH: Deep Learning for the Automated Spectral Classification of Supernovae and their Hosts,” *Astrophys. J.* **885** (2019), 85 [arXiv:1903.02557].
- [75] D. Muthukrishna, G. Narayan, K. S. Mandel, R. Biswas and R. Hložek, “RAPID: Early Classification of Explosive Transients using Deep Learning,” *Publ. Astron. Soc. Pac.* **131** (2019) no.1005, 118002 [arXiv:1904.00014].

- [76] M. Vargas dos Santos, M. Quartin and R. R. R. Reis, “On the cosmological performance of photometric classified supernovae with machine learning,” *Mon. Not. Roy. Astron. Soc.* **497**, no.3, 2974-2991 (2020) [arXiv:1908.04210].
- [77] C. Fremling, X. J. Hall, M. W. Coughlin, A. S. Dahi-wale, D. A. Duev, M. J. Graham, M. M. Kasliwal, E. C. Kool, A. A. Mahabal and A. A. Miller, *et al.* “SNI-ascor: Deep-learning Classification of Low-resolution Supernova Spectra,” *Astrophys. J. Lett.* **917**, no.1, L2 (2021) [arXiv:2104.12980].
- [78] M. Seikel, C. Clarkson and M. Smith, “Reconstruction of dark energy and expansion dynamics using Gaussian processes,” *JCAP* **06** (2012), 036 [arXiv:1204.2832]. GaPP is available at <https://github.com/astrobangaly/GaPP>
- [79] F. Pedregosa *et al.*, “Scikit-learn: Machine Learning in Python,” *Journal of Machine Learning Research* **12** (2011), 2825, <https://scikit-learn.org/stable/index.html>
- [80] L. Breiman, J. Friedman, R. Olshen, and C. Stone, “Classification and Regression Trees’’, Wadsworth, Belmont, (1984).
- [81] D. E. Rumelhart, G. E. Hinton, and R. J. Williams, “Learning representations by back-propagating errors”, *Nature* **323** (1986), 533
- [82] T. Chen and C. Guestrin, “XGBoost: A scalable tree boosting system. arXiv 2016,” [arXiv:1603.02754]. <https://xgboost.readthedocs.io/en/latest/#>
- [83] C. M. Bishop, “Pattern Recognition and Machine Learning”, Springer (2006).
- [84] A. J. Smola and B. Schölkopf, “A tutorial on support vector regression”, *Statistics and Computing* **14** (2004), 199
- [85] T. Padmanabhan, “Do We Really Understand the Cosmos?,” *Comptes Rendus Physique* **18** (2017), 275-291 [arXiv:1611.03505].

Appendix A: Hyperparameter optimisation description

For the Extra-Trees Regressor (EXT) algorithm, we perform a grid search over the following hyperparameters

```
gcv = GridSearchCV(ExtraTreesRegressor
(min_samples_split=2,
random_state=42),
param_grid={
'n_estimators': np.arange(1,100,2),
```

```
'max_depth': np.arange(1,10,2),
cv=3, refit=True)
```

For the Artificial Neural Networks (ANN), our grid search is given by

```
gcv = GridSearchCV(MLPRegressor
(solver='lbfgs', learning_rate='adaptive',
max_iter=200,
random_state=42),
param_grid={'hidden_layer_sizes':
np.arange(10,250,10),
'activation': ["identity", "logistic",
"tanh", "relu"]},
'max_iter': np.arange(100,1000,100)},
cv=3, refit=True)
```

As for the Extreme Gradient Boosting (XGB), the grid search corresponds to

```
gcv = GridSearchCV(xgboost.XGBRegressor
(max_depth=2,
min_samples_split=2,
seed=42),
param_grid={
'n_estimators': np.arange(20,500)},
cv=3, refit=True)
```

While the Support Vector Machine (SVM) grid search is described by

```
gcv = GridSearchCV(SVR(kernel='poly', C=100,
gamma='auto', epsilon=.1,
coef0=1),
param_grid={
'degree': np.arange(1, 10)},
cv=3, refit=True)
```

In order to evaluate the performance of these methods, we report the results of the training and test score as

```
print(gcv.best_estimator_.predict([[0.]]),
gcv.score(z_train, hz_train),
gcv.score(z_test, hz_test))
```

Appendix B: Algorithm performance results

alg	N_z	$H_0 \pm \sigma_{H_0}$	sctr $\pm \sigma_{\text{sctr}}$	scts $\pm \sigma_{\text{scts}}$	BVT
EXT	20	80.075 ± 0.646	1.0000 ± 0.0000	0.9612 ± 0.0100	162.094
	30	74.646 ± 0.552	1.0000 ± 0.0000	0.9968 ± 0.0014	53.396
	50	71.905 ± 0.570	1.0000 ± 0.0000	0.9978 ± 0.0011	20.981
	80	72.107 ± 0.202	1.0000 ± 0.0000	0.9980 ± 0.0007	22.826
ANN	20	64.739 ± 4.595	0.9992 ± 0.0005	0.9933 ± 0.0057	27.986
	30	66.461 ± 2.576	0.9992 ± 0.0004	0.9982 ± 0.0011	7.444
	50	67.090 ± 1.396	0.9991 ± 0.0003	0.9932 ± 0.0007	2.022
	80	66.838 ± 1.317	0.9990 ± 0.0002	0.9985 ± 0.0005	2.008
XGB	20	83.031 ± 0.722	0.9949 ± 0.0017	0.8502 ± 0.0244	271.794
	30	74.743 ± 0.554	0.9998 ± 0.0000	0.9821 ± 0.0053	54.817
	50	72.084 ± 0.531	0.9986 ± 0.0001	0.9903 ± 0.0028	22.602
	80	72.592 ± 0.642	0.9967 ± 0.0001	0.9954 ± 0.0015	27.782
SVM	20	67.879 ± 2.317	0.9989 ± 0.0006	0.9961 ± 0.0036	5.638
	30	67.286 ± 1.169	0.9990 ± 0.0004	0.9984 ± 0.0009	1.373
	50	67.262 ± 0.957	0.9990 ± 0.0003	0.9984 ± 0.0007	0.925
	80	67.244 ± 0.778	0.9989 ± 0.0002	0.9985 ± 0.0005	0.619
GAP SqExp	20	67.178 ± 0.636	-	-	0.437
	30	67.220 ± 0.544	-	-	0.316
	50	67.132 ± 0.481	-	-	0.284
	80	66.135 ± 0.424	-	-	0.230
GAP Mat52	20	67.005 ± 0.721	-	-	0.645
	30	67.027 ± 0.658	-	-	0.544
	50	66.993 ± 0.533	-	-	0.419
	80	67.060 ± 0.530	-	-	0.371

TABLE I: Respectively: H_0 measurements (in units of $\text{kms}^{-1} \text{Mpc}^{-1}$), score-train, and score-test with their respective 1σ uncertainties, as well as the BVT values obtained for all N_z and ML algorithms assuming $\sigma_H/H = 0.008$. We also show the results obtained using the GAP method at the bottom of the table.

alg	N_z	$H_0 \pm \sigma_{H_0}$	sctr $\pm \sigma_{\text{sctr}}$	scts $\pm \sigma_{\text{scts}}$	BVT
EXT	20	80.099 ± 0.729	1.0000 ± 0.0000	0.9586 ± 0.0127	162.084
	30	74.606 ± 0.699	1.0000 ± 0.0000	0.9959 ± 0.0020	52.995
	50	71.705 ± 0.774	1.0000 ± 0.0000	0.9963 ± 0.0016	19.482
	80	72.145 ± 0.234	1.0000 ± 0.0000	0.9971 ± 0.0011	23.378
ANN	20	65.045 ± 6.033	0.9986 ± 0.0012	0.9884 ± 0.0149	41.753
	30	66.274 ± 4.060	0.9988 ± 0.0006	0.9971 ± 0.0018	17.666
	50	66.575 ± 1.566	0.9986 ± 0.0005	0.9973 ± 0.0013	3.069
	80	66.706 ± 1.308	0.9983 ± 0.0003	0.9979 ± 0.0006	2.139
XGB	20	83.678 ± 0.763	0.9952 ± 0.0024	0.8477 ± 0.0322	266.864
	30	74.743 ± 0.554	0.9998 ± 0.0000	0.9821 ± 0.0053	54.292
	50	72.084 ± 0.531	0.9986 ± 0.0001	0.9903 ± 0.0028	21.227
	80	72.592 ± 0.642	0.9967 ± 0.0001	0.9945 ± 0.0017	28.973
SVM	20	67.973 ± 2.230	0.9984 ± 0.0008	0.9946 ± 0.0038	5.352
	30	67.578 ± 1.477	0.9985 ± 0.0006	0.9974 ± 0.0018	2.230
	50	67.215 ± 1.084	0.9990 ± 0.0005	0.9974 ± 0.0012	1.196
	80	67.164 ± 0.979	0.9989 ± 0.0004	0.9979 ± 0.0007	0.996
GAP SqExp	20	67.320 ± 0.893	-	-	0.799
	30	67.198 ± 0.656	-	-	0.457
	50	67.120 ± 0.563	-	-	0.374
	80	66.178 ± 0.459	-	-	0.243
GAP Mat52	20	67.097 ± 0.989	-	-	1.047
	30	66.950 ± 0.723	-	-	0.690
	50	66.930 ± 0.646	-	-	0.601
	80	67.026 ± 0.554	-	-	0.419

TABLE II: Same as Table I, but assuming $\sigma_H/H = 0.01$.

alg	N_z	$H_0 \pm \sigma_{H_0}$	sctr $\pm \sigma_{\text{sctr}}$	scts $\pm \sigma_{\text{scts}}$	BVT
EXT	20	79.961 \pm 2.240	1.0000 \pm 0.0000	0.9241 \pm 0.0440	163.815
	30	74.376 \pm 2.401	1.0000 \pm 0.0000	0.9700 \pm 0.0186	54.997
	50	71.711 \pm 2.118	1.0000 \pm 0.0000	0.9692 \pm 0.0127	23.421
	80	71.787 \pm 2.481	1.0000 \pm 0.0000	0.9747 \pm 0.0091	25.751
ANN	20	63.983 \pm 13.973	0.9873 \pm 0.0083	0.9171 \pm 0.1629	206.656
	30	65.504 \pm 8.225	0.9988 \pm 0.0052	0.9771 \pm 0.1501	71.094
	50	65.928 \pm 5.194	0.9986 \pm 0.0046	0.9973 \pm 0.0013	29.028
	80	64.855 \pm 5.539	0.9848 \pm 0.0038	0.9811 \pm 0.0006	3.695
XGB	20	83.394 \pm 2.326	0.9913 \pm 0.0077	0.8128 \pm 0.0322	262.511
	30	75.805 \pm 2.365	0.9971 \pm 0.0037	0.9549 \pm 0.0231	76.901
	50	72.692 \pm 1.810	0.9963 \pm 0.0022	0.9633 \pm 0.0128	31.699
	80	73.322 \pm 1.938	0.9933 \pm 0.0026	0.9750 \pm 0.0085	39.304
SVM	20	66.692 \pm 6.299	0.9843 \pm 0.0086	0.9563 \pm 0.0304	40.121
	30	66.895 \pm 3.902	0.9857 \pm 0.0055	0.9777 \pm 0.0121	15.440
	50	67.133 \pm 2.614	0.9846 \pm 0.0044	0.9767 \pm 0.0117	6.884
	80	67.073 \pm 2.445	0.9835 \pm 0.0041	0.9818 \pm 0.0078	6.061
GAP SqExp	20	66.980 \pm 2.566	-	-	6.727
	30	66.938 \pm 1.882	-	-	3.721
	50	67.090 \pm 1.460	-	-	2.203
	80	66.859 \pm 1.422	-	-	2.274
GAP Mat52	20	66.640 \pm 2.376	-	-	6.164
	30	66.508 \pm 1.798	-	-	3.957
	50	66.633 \pm 1.406	-	-	2.463
	80	66.403 \pm 1.355	-	-	2.752

TABLE III: Same as Table I, but assuming $\sigma_H/H = 0.03$.

alg	N_z	$H_0 \pm \sigma_{H_0}$	sctr $\pm \sigma_{\text{sctr}}$	scts $\pm \sigma_{\text{scts}}$	BVT
EXT	20	80.454 \pm 3.847	1.0000 \pm 0.0000	0.8358 \pm 0.1445	186.254
	30	74.439 \pm 3.963	1.0000 \pm 0.0000	0.9210 \pm 0.0409	65.821
	50	71.937 \pm 3.771	1.0000 \pm 0.0000	0.9186 \pm 0.0330	35.171
	80	72.037 \pm 3.454	0.9997 \pm 0.0002	0.9268 \pm 0.0273	33.809
ANN	20	67.822 \pm 22.801	0.9654 \pm 0.0214	0.6345 \pm 1.6201	520.117
	30	64.957 \pm 13.282	0.9660 \pm 0.0188	0.9307 \pm 0.0417	182.184
	50	66.324 \pm 6.833	0.9637 \pm 0.0127	0.9349 \pm 0.0303	47.758
	80	67.051 \pm 7.688	0.9588 \pm 0.0104	0.9471 \pm 0.0191	59.196
XGB	20	83.515 \pm 3.211	0.9767 \pm 0.0197	0.7389 \pm 0.1639	271.267
	30	76.861 \pm 3.045	0.9858 \pm 0.0122	0.9061 \pm 0.0491	99.536
	50	73.469 \pm 3.012	0.9841 \pm 0.0088	0.9201 \pm 0.0316	46.389
	80	74.472 \pm 2.554	0.9933 \pm 0.0026	0.9750 \pm 0.0085	57.112
SVM	20	66.907 \pm 8.859	0.9559 \pm 0.0222	0.8713 \pm 0.1073	78.695
	30	66.678 \pm 5.348	0.9591 \pm 0.0180	0.9378 \pm 0.0331	29.066
	50	66.891 \pm 4.492	0.9598 \pm 0.0134	0.9327 \pm 0.0315	20.399
	80	67.212 \pm 3.541	0.9557 \pm 0.0105	0.9485 \pm 0.0181	12.561
GAP SqExp	20	66.817 \pm 3.789	-	-	14.649
	30	66.313 \pm 3.524	-	-	13.512
	50	66.612 \pm 2.558	-	-	7.103
	80	66.896 \pm 2.464	-	-	6.284
GAP Mat52	20	66.573 \pm 3.252	-	-	11.977
	30	66.188 \pm 3.149	-	-	11.293
	50	66.250 \pm 2.343	-	-	6.723
	80	66.355 \pm 2.150	-	-	5.631

TABLE IV: Same as Table I, but assuming $\sigma_H/H = 0.05$.

alg	N_z	$H_0 \pm \sigma_{H_0}$	sctr $\pm \sigma_{\text{sctr}}$	scts $\pm \sigma_{\text{scts}}$	BVT
EXT	20	79.882 ± 6.367	1.0000 ± 0.0000	0.6492 ± 0.3092	197.350
	30	74.182 ± 6.158	1.0000 ± 0.0000	0.8028 ± 0.1082	84.454
	50	72.566 ± 5.484	1.0000 ± 0.0000	0.7963 ± 0.1015	57.175
	80	72.037 ± 5.560	0.9994 ± 0.0002	0.9268 ± 0.0273	33.809
ANN	20	64.344 ± 32.581	0.9231 ± 0.0508	0.3635 ± 1.2179	1070.650
	30	65.562 ± 20.622	0.9195 ± 0.0378	0.7984 ± 0.2145	428.461
	50	67.091 ± 7.667	0.9124 ± 0.0265	0.8548 ± 0.0774	58.861
	80	65.274 ± 8.579	0.9044 ± 0.0182	0.8636 ± 0.0659	81.072
XGB	20	82.232 ± 4.713	0.9439 ± 0.0513	0.6266 ± 0.3210	243.402
	30	77.114 ± 4.405	0.9539 ± 0.0284	0.8211 ± 0.0971	114.544
	50	74.998 ± 3.443	0.9489 ± 0.0199	0.8271 ± 0.0852	70.201
	80	75.144 ± 3.145	0.9362 ± 0.0161	0.8513 ± 0.0607	70.489
SVM	20	66.609 ± 11.299	0.8928 ± 0.0585	0.7287 ± 0.2258	128.228
	30	67.710 ± 7.386	0.9034 ± 0.0372	0.8491 ± 0.0854	54.677
	50	66.395 ± 6.126	0.9039 ± 0.0258	0.8541 ± 0.0721	38.456
	80	66.950 ± 5.313	0.8998 ± 0.0175	0.8642 ± 0.0610	28.399
GAP SqExp	20	64.727 ± 5.818	-	-	40.786
	30	65.934 ± 4.915	-	-	26.189
	50	66.578 ± 4.419	-	-	20.143
	80	66.813 ± 3.194	-	-	10.450
GAP Mat52	20	65.334 ± 5.284	-	-	32.079
	30	66.206 ± 4.717	-	-	23.575
	50	66.418 ± 3.942	-	-	16.425
	80	66.369 ± 2.921	-	-	9.512

TABLE V: Same as Table I, but assuming $\sigma_H/H = 0.08$.